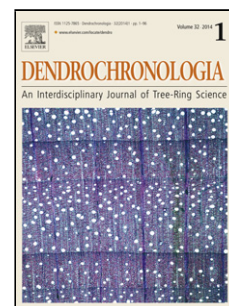# Accepted Manuscript

Title: Animating tree colonization and growth

Author: <ce:author id="aut0005"
author-id="S1125786516301734-
12a949b2a402c40ad9a117b7dcb1fa22"> Jonathan G.A.
Lageard<ce:author id="aut0010"
author-id="S1125786516301734-
8eba1632b272309dda24bfec10b7afe5"> Peter A.
Thomas<ce:author id="aut0015"
author-id="S1125786516301734-
43aaf2215f6c9a7ae5364f5329471702"> Jianquan
Cheng

Please cite this article as: Lageard, Jonathan G.A., Thomas, Peter A.,
Cheng, Jianquan, Animating tree colonization and growth.Dendrochronologia
http://dx.doi.org/10.1016/j.dendro.2016.11.006

Technical Note

Animating tree colonization and growth

Jonathan G.A. Lageard [a], Peter A. Thomas [b], Jianquan Cheng [a]

[a]Division of Geography and Environmental Management, School of Science and the Environment, Manchester Metropolitan University, Chester Street, Manchester, M1 5GD, UK

[b] School of Life Sciences, Keele University, Staffordshire ST5 5BG, UK.

Abstract

In the early twentieth century the woodland at Heald Brow, north-west England, was largely a tree-less pasture, but changing land management practices lead to natural tree colonization and the development of a mixed deciduous woodland with ash (*Fraxinus excelsior*), oak (*Quercus robur*), yew (*Taxus baccata*) and small-leaved Lime (*Tilia cordata*) the main components. The research focused on *T. cordata* due to its rarity and conservation value, and aimed to investigate the timing of its appearance, rates of reproduction by layering and the effects of competition on its longer-term survival. A small, 0.32 ha area of woodland was mapped using standard field-based survey methods and increment cores were taken to provide minimum age estimates for living stems of all species present. The spatial and temporal data generated led to the development of a new micro-GIS animation method, using ArcGIS software, that visually highlighted secondary woodland establishment and development, and gave novel insights into the competitive interactions that governed the development. Results showed *T. cordata* colonization in the 1940s and layering developing in the 1960s. The later appearance and rapid establishment of *T. baccata* with its light-excluding canopy produced high competition scores and undoubtedly restricted further development of the main *T. cordata* canopy aided by *F. excelsior* at the periphery. This animation method and associated GIS analyses have potential application in both dendrochronological, wider ecological research and in conservation management.

Key words: animation, competition, micro-GIS, tree colonization, tree growth.

Introduction

Environmental change and the effects of human activity have been successfully demonstrated using techniques including pollen and associated analyses such as quantification of micro and macroscopic charcoal (Branch and Marini, 2014), but only dendrochronology can provide precise chronological records. This is demonstrated by studies of ecesis, the interval between ground exposure and tree colonisation, such as tree colonisation of glacier forefields (Luckman, 1988), of debris-covered glaciers (Pelfini et al., 2007), of terrain following volcanic activity (Yamaguichi et al., 1990) or of abandoned land following changes in the intensity of agricultural practices (Schöne and Schweingruber, 2001).

As woodlands and forests become established, competition and disturbance are key factors affecting the nature and composition of these ecosystems (Whitmore, 1990; Peterken, 1993; Thomas & Packham 2007), and have been the focus of many dendrochronological studies, for instance in assessments of disturbance (Čada et al., 2013; Druckenbrod et al., 2013; Pavel et al., 2015). Indeed, it has been argued that the impact of competition as a factor in long-term forest change may often be under-estimated (Büntgen and Schweingruber, 2010; Zhang et al., 2015), and competition indexes are now widely used for interpreting and summarising the intensity, effects and outcomes of plant competition (Weigelt and Jolliffe, 2003). Competition is a primary factor in all ecosystems and is therefore important in contemporary conservation management (Montesinos and Fabado, 2015), particularly under climate change scenarios (Fernández-de-Uña et al., 2015).

Reconstructing forest composition and dynamics has become imperative since the Kyoto agreement on climate change, with the need to quantify and predict forest biomass to calculate carbon sequestration by trees and their role in mitigating rising atmospheric CO_2 concentrations (Krejza et al., 2015). Techniques employed in these reconstructions have included: calculations of tree basal area over time and development of tree-growth models (Krejza et al., 2015), the differentiation of individual tree crowns from remotely-sensed data (Wulder et al., 2000; Leckie et al., 2005; Hurschmugl et al., 2007; Skurikhin et al., 2013) and most recently the use of unmanned aerial vehicles (UAVs) to develop precise plan and oblique view 3-dimensional models of trees and groups of trees (Gatziolis et al., 2015).

In the last decade, analysis of spatial patterns in plant communities has received increasing attention within ecological and particularly forest-related research. Fine-scale spatial structures are mapped and analysed at a range of spatial scales (Felinks and Wiegand 2008; Wiegand et al. 2009), in both tropical and temperate environments (Wiegand et al 2007; Martínez et al., 2010; Miao et al., 2014; Velázquez et al. 2016), to better understand how dominant species coexist and the processes / factors affecting species distribution (Gretzin et al. 2006; Cousens et al. 2008; Punchi-Manage et al. 2016). Pattern analysis has become increasingly sophisticated using statistical approaches e.g. Ripley's K Function (Wiegand and Moloney 2004), although recent research comparing eight different approaches warns that key spatial detail could be missed through the application of single statistical methods in isolation (Wiegand et al. 2013).

Detailed spatial reconstructions and analyses often however only illustrate snap shots of forested areas in a particular year/s, or at a series of census points. The research presented here, in contrast, provides a novel approach in using consecutive, annual spatial snapshot data to produce a GIS-assisted animation and to facilitate related analyses that can rapidly visualize secondary woodland development, subsequent competition and woodland dynamics.

Materials and methods

Description of the site

Heald Brow is an area of pasture and mixed secondary woodland on the northern shores of Morecombe Bay, north-west England, UK (Figure 1), that has developed on limestone pavement and thin calcareous soils following changes in agricultural land use during the twentieth century.   The land slopes gently southwards towards the sea and the most common tree species are (*Fraxinus excelsior* L.) and yew (*Taxus baccata* L.), with oak (*Quercus robur* L.) and small-leaved Lime (*Tilia cordata* Mill.) less frequent (Figure 2).

Research rationale

The land is owned by the National Trust and their land management focuses on enhancing biodiversity and promoting native species such as *T. cordata*, which as elsewhere in the UK is rare and regarded as a species of conservation significance (Logan et al., 2015). The present-day climate of Heald Brow does not allow reproduction of *T. cordata* from seed, and consequently clonal spreading or layering (Pigott 1991) is the dominant regeneration process. Consequently, this research was designed to quantify rates of *T. cordata* layering and to assess the species survival chances within the longer-term development of the woodland.

The research concentrated on one specific cluster of larger *T. cordata* stems and their smaller clonal progeny linked by ground-hugging branches radiating from the central group (Figure 2). The aim of this study was to record and date all the original and layered *T. cordata* stems that formed one continuous central canopy, but also to record similar data for surrounding individuals of other tree species in order to study rates of secondary woodland colonization and subsequent inter-species competition. This presented an opportunity to develop a novel micro-GIS method to better visualize spatially-referenced woodland records. This technique is the primary focus of this Technical Note.

Description of the field and laboratory methods

A small c. 3200 m^2 (0.32 ha) area was defined around a central cluster of *T. cordata* stems forming one unbroken canopy, with the aim of reconstructing its longer-term dynamics and those of the surrounding woodland. A relatively small sampling area was chosen, containing 59 living tree stems, to test the viability of whether woodland dynamics could be visualized using small scale or micro-GIS animation.

Stem locations could not be recorded with high positional accuracy using an EDM (Electronic Distance Measuring) device or using other recent advances in mapping (Bowie et al. 2014) due to the dense nature of the woodland and the rugged topography (see Figure 2).   The positional accuracy of Global Positioning Systems (GPS) or differential GPS was also insufficient to accurately separate stems growing in some cases less than 1m apart. As a result, more traditional ground survey techniques were employed (cf Ritchie et al., 1988) to create a plan view map of stem locations (Figure 3). To produce this map, a point was chosen within the central cluster of *T. cordata* stems from which all measurements to individual stems were made using a 30m tape (cf Martínez et al., 2010; Miao et al., 2014).   For each stem, a compass bearing from north was taken from the central reference point; circumference was measured at 0-0.5 m above ground; and a 5mm increment core was removed at *c*. 30 cm above ground using a Pressler-type increment borer.

A similar method was used to record the location, size and age of ash (*F. excelsior*), yew (*T. baccata*) and oak (*Q. robur*) stems surrounding the central *T. cordata* cluster. The spatial extent of the canopy of all trees measured was estimated in order to record current canopy interactions between *T. cordata* and surrounding species. The outer edges of each canopy were recorded where they over-laid the tape measure stretched between the central reference point and the tree in question. An initial base map was drawn manually including stem locations and estimated canopy extents.

3

Tree increment cores were dried and prepared using standard techniques (Schweingruber, 1988; Speer 2010). Measurements of annual ring-widths were made using a measuring stage and software (Input and Dendro © Tyers 1999) as described by Lageard et al. (1999). Resultant data for each tree included number of annual rings at *c.* 30 cm above the ground (no correction was made for sampling height), and estimated year of germination (minimum estimate / samples were not taken from trunk base). The latter included interpolated age ranges where the pith had been missed during coring. Reported ages therefore represent under-estimates of true calendar dates for germination / colonisation but allow a relative comparison between stems. Where a single 'year of germination' could not be specified, a mid-point in the estimated calendar age range was used in the GIS analyses reported below.

Description of the GIS method

With all spatial and temporal data available for trees in the study area, it was then possible to produce a temporal animation depicting tree germination and subsequent radial growth over time. This animation involved the step-by-step application of the following GIS method.

Step 1: Defining a coordinator system

A plain coordinate system, defined by a boundary (0, 0) and (170m, 45m) was established to contain the *T. cordata* cluster at its centre and surrounding *F. excelsior*, *T. baccata* and *Q. robur* individuals. The coordinates of the four corners were typed into Microsoft Excel and saved as a CSV file.

Step 2. Digitizing tree stem locations and editing their attribute data

A map was drawn manually and subsequently all stem locations in the survey area were digitised, each located with a point. A point layer was created in ArcGIS 10.3.1 using the *display XY* tool and the dimensions identified in Step 1, and the digitised points were imported using the *Editor* tool. Attribute data, including estimated year of germination and stem circumference, were typed into an attribute table.

Step 3.

To animate tree growth over time, tree circumference was estimated for each year that the tree was alive from estimated germination to year of sampling. For simplicity, it was assumed that tree stem circumference followed a linear growth trend.

$$C(i)_Y = A(i) *Y \qquad (1)$$

Where $C(i)_Y$ is the stem circumference at location *i* in year *y* and a(*i*) is a parameter for the tree at location *i*. [Actual ring-width measurements could alternatively be used].

A short program in vb.net together with the freeware dotspatial (www.dotspatial.com; free GIS mapping components) was developed to copy the location of each tree for all the years from its germination year (e.g. AD 1931 until AD 2011) – see Additional Materials. The attribute data stayed the same whilst stem circumference was updated for each successive year according to the value calculated in equation 1.

$$S(i)_Y = 2+(2012 - y_0) \times C(i)_Y/C(i) \qquad (2)$$

Where $S(i)_y$ is the point size at location *i* for year *y*, y_0 is the year of germination, and $C(i)$ is the stem circumference at location *i* in the surveyed year (e.g. AD 2011); and $C(i)y$ from equation 1.

4

The point layer in Step 2 was up-dated to create 3,109 records (or points) in the case study presented here. Another purpose of this was to allocate a point symbol to represent stem circumference size reached during each year of the study period. These sizes ranged from values of 2 to 20 (0 and 1 symbol sizes were not used as they were too small for meaningful visualization). Further, 20 was chosen as the upper limit to avoid point symbols being too large and overlapping. Similar scaling of proportional symbols has been successfully employed elsewhere (Murdock et al 2012).

Step 4: Creating an animation file

As the updated point layer had a field labelled 'Year', ranging from AD 1906 to AD 2011, the animation (using the *Animation* tool, or the *Time Slider* icon in ArcGIS 10.3.1), could show 106 layers (or snapshots) continuously. To display the changing stem circumferences, the point size for the point symbols was defined by the estimated variable $C(i)_y$ in equation (2). The animation was saved as an avi file for the animation presentation [see Additional Materials].

Step 5: Creating a snapshot of stem growth (circumference)

The attribute table of the point layer created at Step 3 had an estimated point symbol size for each year at each surveyed location. Using *Selection by Attribute* (ArcGIS 10.3.1), records for an individual year could be selected and exported into a separate point layer, named individually e.g. AD 1906. To ensure a consistent legend for each point layer (each year or each snapshot), the *Apply Symbology to Multi* tool was employed to set a same symbology for all point layers.

Step 6: Calculating degree of competition

The degree of competition experienced by each tree can be expressed in terms of intensity values (cf Anning and McCarthy, 2013) using the following formula:

$$CI\ (i) = \sum_{j=1}^{n} \frac{C(j)/C(i)}{dij} \qquad (3)$$

Where CI(*i*) is the competition index calculated for location *i*, C(*j*) is the stem circumference at location *j* and C(*i*) at location *i*, and d*ij* is the Euclidean distance between location *i* and *j*. *n* is the total number of locations across the study area.

Step 7: Further micro GIS analysis

Further micro GIS analysis can demonstrate otherwise unseen patterns in the spatial data. Kernel density analysis (KDA available in ArcGIS 10.3.1) for instance, as a visual tool, is a popular method for exploring hot spot areas based on point type data (see Figure 8). It uses a moving kernel function to weight points within a search neighbourhood according to their distance to a specific location where density is being calculated. The extent of smoothing on the created surface is dependent on the user-defined bandwidth of the kernel, which reflects the scale of analysis being undertaken.

Results

Animation

The animation resulting from the Heald Brow study site (see Additional Materials) included data on 59 tree stems from an area of a little less than 3200 m^2 (0.32 ha). The earliest estimated year of germination was A.D. 1906 (*F. excelsior*) and the animation covered the period until AD 2011.

5

Key phases of the animation for this particular case study are illustrated by the stem circumference snapshots in Figure 4 (see Step 5 above), illustrating initial colonization by *F. excelsior* shortly followed by *T. cordata* establishment in the 1940s and the central *T. cordata* stem cluster developing in the 1950s. More dense woodland is present from the 1960s including the first appearance of *T. baccata*, the latter quickly establishing in the next 20 years. Vegetative regeneration by *T. cordata* appears to commence in the 1960s with this process accelerating in the 1980s and 1990s, clearly and quickly visualized in the animation. In addition to general trends in secondary colonization it is also possible to gauge inter-species competition in selected parts of the area, for instance to view interactions between peripheral *T. cordata* and later-appearing *F. excelsior* and *T. baccata* (see section below).

Micro-GIS analyses

Spatially-referenced data from this study can also be subjected to both standard and also more complex GIS analyses. The Euclidean distance between a tree and its nearest neighbour can easily be calculated using the *spatial join* tool in ArcGIS 10.3.1. In the case of the Heald Brow woodland in AD 2011 the minimum distance between all trees was 0.42 m, with the maximum distance 6.42m and mean distance 1.84m, facilitating stand or species density calculations during the study period. Other simple data analyses that can be undertaken include visualizing the occurrences of initial colonists and also of more recent sapling establishment (germination years - Figure 5), and also calculating average growth rates of all the trees (Figure 6).

The power of this micro-GIS application is not just in these basic analyses, but also in more subtle data manipulations that can provide some spatial insight into ecological processes. Two thematic maps demonstrate the spatial distributions of stem circumferences in the survey year A.D. 2011 (Figure 7a) and the same data viewed using the Kernel Density analysis tool to highlight spatially significant trends (Figure 7b). The west-east pattern highlighted in Figure 7b does not follow any obvious linear patterns on the ground (the grykes, small valleys in the limestone pavement, trend south-south-west to east-north-east) and these data therefore deserve more in-depth analysis and explanation.

Competition, as calculated by Anning and McCarthy 2013, between trees in the study in AD 2011 is illustrated in Figure 8. This diagram demonstrates that despite their later appearance during secondary woodland development, *T. baccata* individuals quickly become established, exerting a significant physical presence, with their light-excluding canopies placing them at a competitive advantage. The highest competition scores in AD 2011 are recorded for *F. excelsior* and *T. cordata* stems particularly those close to the *T. cordata* outer canopy edge. It would be possible to calculate competition scores for every stem during each year of the study and to re-run the animation to record spatial variations in competition during the period AD 1906 – 2011.

Rate of layering and conservation significance

The aim of this paper is to highlight a novel approach using micro-GIS analyses to make broader spatial interpretations of data resulting from dendroecological and ecological / forestry research. The detailed implications of data from Heald Brow, rates of layering in *T. cordata* and conservation significance will be presented elsewhere.

Discussion.

Mainstream GIS applications have been used with some success in ecological, dendrochronological and other subject areas to analyse variables at large-, intermediate- and some relatively small-scales (Stoffel et al., 2005; Goodchild, 2011; Boyd and Foody, 2011). Examples of small scale or micro-GIS studies are

however still rare, often confined to areas other than ecology, such as the built environment (Hilton and Burkhard, 2009). An important exception has been the use of GIS in wood anatomical studies (Latte et al., 2015).

The research reported here employed standard surveying and dendrochronological techniques to establish rates of layering in *T. cordata*, and to examine competition between *T. cordata* and other key components (*F. excelsior*, *T. baccata*, *Q. robur*) of surrounding secondary woodland, in a small 0.32 ha study area. The subsequent application of a novel GIS animation and associated GIS analyses has demonstrated that such visualizations of tree colonization and subsequent interactions / competition can provide a novel and important fine–resolution temporal window into understanding the nature and rates of ecological change.

Other ecological research could also benefit from temporal data animation, for instance mapping and following the impacts of invasive species (cf Knüsel et al., 2015), or assessing the relative merits of seed dispersal agents (Qiu et al., 2008). Qui et al. for example use static snapshots from the 250-year simulation using a GIS-based theoretical model to assess the relative importance of wind, gravity, water and animals.

The analysis of spatial patterns in plant communities has been a rapidly-developing recent research area, but despite increasing levels of statistical sophistication (cf. Wiegand et al. 2013), interpretations are often also based on temporal snap shots or series of census points, with findings at times appearing inconclusive. Martínez et al. for instance used spatial point pattern analysis on a small temperate forest plot, identifying a series of consecutive processes that 'could influence the current tree distribution pattern…' (Martínez et al. 2010: 456). Miao et al. employ similar detailed analyses in a 4 ha forest study plot to study the spatial influence of remnant trees following disturbance events on the Tibetan Plateau (Miao et al., 2010: 107). Analyses of a series of consecutive annual snapshots included in a GIS animation (Miao et al undertook a detailed quadrat-based survey in one calendar year) might however provide a clearer picture of more subtle spatial changes relating to shade-intolerant species following disturbance events.

Dendrochronological research has also been able to investigate forest disturbance, providing temporal clarity on the nature and timing of disturbance events. Models of woodland development generated by such studies (cf Druckenbrod et al. 2013), could be tested using the new GIS animation exemplified in this paper. Further potential applications of GIS animation include in 3D models of woodland dynamics, where data capture is focussed not only on horizontal, but also vertical reconstructions using techniques such as LIDAR (Rosell et al., 2009; Vepakomma et al., 2011; Hosoi et al., 2013) and also where dendrochronological data informs conservation management (Gea-Izquierdo et al., 2015).

Dendrochronology continues to evolve as a discipline, encompassing analyses of annual growth not only in trees, but also shrubs, dwarf shrubs and perennial herbs (cf Schweingruber & Buntgen 2013). Research in these areas provides further justification, not only for focussing on smaller scale study sites, but also on the development of new tools for data visualization such as micro-GIS animation.

Conclusion

A detailed survey of secondary woodland focussing on *T. cordata* has shown how data collected through standard ground survey and dendrochronological techniques can be animated and used to gain better understanding of rates of colonisation and in visualising woodland competition. This novel use of micro-GIS has broad application, both within dendrochronology and in wider ecological research.

References

Anning, A. K., McCarthy, B.C., 2013. Competition, size and age affect tree growth response to fuel reduction treatments in mixed-oak forests of Ohio. Forest Ecology and Management 307, 74–83.

Boyd, D.S., Foody, G.M., 2011. An overview of recent remote sensing and GIS based research in ecological informatics. Ecological Informatics 6, 25–36.

Bowie, G.D., Millward, A.A., Bhagat, N.N., 2014. Interactive mapping of urban tree benefits using Google Fusion Tables and API technologies. Urban Forestry and Urban Greening 13(4), 742-755.

Branch, N.P., Marini, N.A.F., 2014. Mid-Late Holocene environmental change and human activities in the northern Apennines, Italy. Quaternary International 353, 34-51.

Büntgen, U., Schweingruber, F.H., 2010. Environmental change without climate change? New Phytologist 188, 646–651.

Čada, V., Svoboda, M., Janda, P., 2013. Dendrochronological reconstruction of the disturbance history and past development of the mountain Norway spruce in the Bohemian Forest, central Europe. Forest Ecology and Management 295, 59‑68.

Cousens R. D., Wiegand T. and Taghizadeh M. S. 2008. Small-Scale Spatial Structure within Patterns of Seed Dispersal. Oecologia Vol. 158 (3), 437-448.

Druckenbrod, D.L., Pederson, N., Rentch, J., Cook, E.R., 2013. A comparison of times series approaches for dendroecological reconstructions of past canopy disturbance events. Forest Ecology and Management 302, 23–33.

Felinks B. and Wiegand T. 2008.   Exploring Spatiotemporal Patterns in Early Stages of Primary Succession on FormerLignite Mining Sites. Journal of Vegetation Science 19 (2), 267-276.

Fernández-de-Uña, L., Cañellas, I., Gea-Izquierdo, G., 2015. Stand Competition Determines How Different Tree Species Will Cope with a Warming Climate. PLoS ONE 10(9), e0137932.

Gatziolis, D., Lienard, J.F., Vogs, A., Strigul, N.S., 2015. 3D Tree Dimensionality Assessment Using Photogrammetry and Small Unmanned Aerial Vehicles. PLoS ONE 10(9), e0137765.

Gea-Izquierdo, G., Montes, F., Gavilán, R.G., Cañellas, I., Rubio, A., 2015. Is this the end? Dynamics of a relict stand from pervasively deforested ancient Iberian pine forests. European Journal of Forest Research 134: 525–536.

Goodchild, M.F., 2011. Scale in GIS: An overview, Geomorphology 130(1-2), 5–9.

Getzin S., Dean C., He F., Trofymow J.A., Wiegand K. and Wiegand T. 2006. Spatial Patterns and Competition of Tree Species in a Douglas-Fir Chronosequence onVancouver Island. Ecography 29 (5), 671-682.

Hilton, B., Burkhard, R., 2009. Microenvironment Analysis of a University Campus: GIS Design Considerations for Process Repeatability. Journal of Maps 5(1), 219-231.

Hirschmugl, M., Ofner, M., Raggam, J., Schardt, M., 2007. Single tree detection in very high resolution remote sensing data. Rem Sens Env 110(4): 533–544.

Hosoi, F., Nakai, Y., Omasa, K., 2013. 3-D voxel-based solid modeling of a broad-leaved tree for accurate volume estimation using portable scanning lidar. ISPRS Journal of Photogrammetry and Remote Sensing 82, 41–48.

Knüsel S., Conedera M., Rigling A., Fonti P., Wunder J., 2015. A tree-ring perspective on the invasion of *Ailanthus altissima* in protection forests. Forest Ecology and Management 354, 334-343.

Krejza, J., Svetlık, J., Pokorny, R., 2015. Spatially explicit basal area growth of Norway spruce. Trees 29, 1545–1558.

Lageard, J.G.A., Chambers, F.M., Thomas, P.A., 1999. Climatic significance of the marginalisation of Scots pine (*Pinus sylvestris* L.) circa 2500 BC at White Moss, south Cheshire, UK. The Holocene 9, 321-332.

Latte, N., Beeckman, H., Bauwens, S., Bonnet, S., Lejeune, P., 2015. A novel procedure to measure shrinkage-free tree-rings from very large wood samples combining photogrammetry, high-resolution image processing, and GIS tools. Dendrochronologia 34, 24–28.

Leckie, D.G., Gougeon, F.A., Tinis, S., Nelson, T., Burnett, C.N., Paradine, D., 2005. Automated tree recognition in old growth conifer stands with high resolution digital imagery. Rem Sens Env 94(3), 311–326.

Logan, S.A., Phuekvilai, P., Wolf, K., 2015. Ancient woodlands in the limelight: delineation and genetic structure of ancient woodland species *Tilia cordata* and *Tilia platyphyllos* (Tiliaceae) in the UK. Tree Genetics & Genomes 11: 52.

Luckman, B.H., 1988. Dating the moraines and recession of Athabasca and Dome Glaciers, Alberta, Canada. Arctic & Alpine Research 20(1), 40-54.

Martínez, I., Wiegand, T., González-Taboada, F., Obeso, J. R., 2010. Spatial associations among tree species in a temperate forest community in North-western Spain, Forest Ecology and Management 260, 456–465.

Murdock, M.J., Roth, R.E., Maziekas, N.V., 2012. The Basic Ordnance Observational Management System: geovisual exploration and analysis of improvised explosive device incidents. Journal of Maps, 8(1),120-124.

Miao, N., Liu, S., Yu, H., Shi, Z., Moermond, T., Liu, Y., 2014. Spatial analysis of remnant tree effects in a secondary Abies-Betula forest on the eastern edge of the Qinghai–Tibetan Plateau, China, Forest Ecology and Management, 313, 104–111.

Montesinos, D., Fabado, J., 2015. Changes in land use and physiological transitions of a *Juniperus thurifera* forest: from decline to recovery. Canadian Journal of Forest Research 45(6), 764-769.

Thomas, P.A., Packham, J.R., 2007. Ecology of Woodlands and Forests. Cambridge University Press, Cambridge, pp544.

Pavel S., Lukas K., Ivana, V., 2015. Uncertainty in detecting the disturbance history of forest ecosystems using dendrochronology. Dendrochronologia 35, 51-61.

Peterken, G., 1993. Woodland Conservation and Management 2nd Edition. London, Chapman & Hall pp374.

Pelfini, M., Santilli, M., Leonelli, G., Bozzoni, M., 2007. Investigating surface movements of debris-covered Miage Glacier, Western Italian Alps, using dendroglaciological analysis. Journal of Glaciology 53(180), 141-152.

Pigott , C.D., 1991. Biological Flora of the British Isles: *Tilia Cordata* Miller. Journal of Ecology, 79, 1147-1207.

Preavosto, B., Curta, T., Gueugnot, J., Coquillard, P., 2000. Modeling mid-elevation Scots pine growth on a volcanic substrate. Forest Ecology and Management 131: 223-237.

Punchi-Manage R., Getzin S., Wiegand T., Kanagaraj R., Savitri Gunatilleke C.V., Nimal Gunatilleke I.A.U., Wiegand K. and Huth A. 2013. Effects of topography on structuring local species assemblages in a Sri Lankan mixed dipterocarp forest. Journal of Ecology 101, 149–160.

Qiu, F., Li, B., Chastaina, B., Alfarhana, M.,2008. A GIS based spatially explicit model of dispersal agent behaviour. Forest Ecology and Management, 254(3), 524–537.

Ritchie, W., Wood, M., Wright, R., Tait, D., 1988. Surveying and mapping for field scientists. Longman Scientific & Technical, Harlow, pp180.

Rosell, J.R., Llorens, J., Sanz, R., Arno´, J., Ribes-Dasi, M., Masip, J., Escola`, A., Camp, F., Solanelles, F., Gra`cia, F., Gil, E., Val, L., Planas, S., Palacı´n, J., 2009. Obtaining the three-dimensional structure of tree orchards from remote 2D terrestrial LIDAR scanning. Agricultural and Forest Meteorology, 149, 1505–1515.

Schöne, B.R., Schweingruber, F.H., 2001. Dendrochronologische Untersuchungen zur Verwaldung der Alpen am Beispiel eines inneralpinen Trockentals (Ramosch, Unterengadin, Schweiz). Botanica Helvetica 111/2, 151-168.

Schweingruber, F.H., 1988. Tree Rings: basics and applications of dendrochronology. Dordrecht Reidel, 276 pp.

Schweingruber, F.H. and Büntgen U. 2013. What is 'wood' – An anatomical re-definition. Dendrochronologia 31, 187-191.

Skurikhin, A.N., Garrity, S.R., McDowell, N.G., Cai, D.M., 2013. Automated tree crown detection and size estimation using multi-scale analysis of high-resolution satellite imagery. Remote Sensing Letters 4(5), 465–474.

Stoffel, M., Schneuwly, D., Bollschweiler, M., Lie`vre, I., Delaloye, R., Myint M., Monbaron, M., 2005. Analyzing rockfall activity (1600–2002) in a protection forest—a case study using dendrogeomorphology. Geomorphology 68 , 224– 241.

Velázquez E., Kazmierczak M. and Wiegand T. 2016. Spatial patterns of sapling mortality in a moist tropical forest: consistency with total density-dependent effects. Oikos 125, 872–882.

Vepakomma, U., St-Onge, B., Kneeshaw, D., 2011. Response of a boreal forest to canopy opening: assessing vertical and lateral tree growth with multi-temporal lidar data.   Ecological Applications, 21(1), 99-121.

Weigelt, A., Jolliffe, P., 2003. Indices of plant competition. Journal of Ecology 91(5), 707–720.

Whitmore, T.C., 1990. An introduction to Tropical Rain Forests. Claredon, Oxford pp226.

Weigand T. and Moloney K.A. 2004. Rings, circles, and null-models for point pattern analysis in ecology. OIKOS 104, 209-229.

Wiegand T., He F. and Hubbell S.P. 2013. A systematic comparison of summary characteristics for quantifying point patterns in ecology. Ecography 36, 92–103.

Wiegand T., Gunatilleke S. and Gunatilleke N. 2007. Species Associations in a Heterogeneous Sri Lankan Dipterocarp Forest.   The American Naturalist 170 (4) 77-95.

Wiegand T., Martínez I. and Huth A. 2009. Recruitment in Tropical Tree Species: Revealing Complex Spatial Patterns. The American Naturalist 174 (4), 106-140.

Wulder, M., Niemann, K.O., Goodenough, D.G., 2000. Local maximum filtering for the extraction of tree locations and basal area from high spatial resolution imagery. Rem. Sens. Env. 73, 103–114.

Yamaguichi, D.K., Hoblitt, R.P., Lawrence, D.B., 1990. A new tree-ring date for the 'Floating Island' lava flow, Mt St. Helens, Washington.   Bulletin of Volcanology 52, 545-550.

Zhang, J., Huang, S., He, F., 2015. Half-century evidence from western Canada shows forest dynamics are primarily driven by competition followed by climate. Proceedings of the National Academy of Science (USA) 112(13), 4009–4014.

List of Figures

Figure 1. Location of the Heald Brow study area at the northern end of Morecombe Bay, north Lancashire, UK (Images: Digimap:© Crown copyright/database right 2010. An Ordnance Survey/EDINA supplied service and © Google Earth, May 2009).

Figure 2. A cluster of *Tilia cordata* stems growing on limestone pavement at Heald Brow. Evidence of vegetative regeneration or layering can be seen on the right of the image in the low growing connected branch (Image: February 2012).
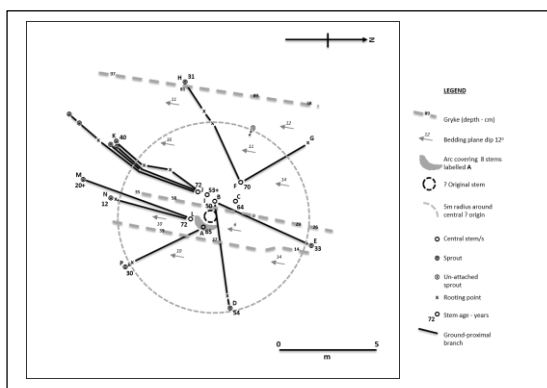

Figure 3. Ground survey map of *T. cordata* stems, illustrating seven central older individuals (oldest minimum estimate 72 years) and younger layered progeny located c. 5m from the centre of the clonal grouping.
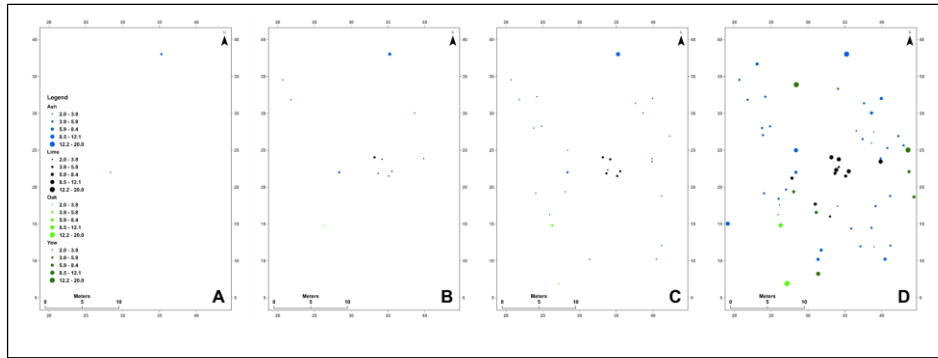
Figure 4A-D. Stem circumference snap shots (created using STEP 5 outlined in the Method) illustrating tree colonization and subsequent stem growth at key intervals: A - AD 1910, B – AD 1950, C – AD 1960, D - AD 2000.
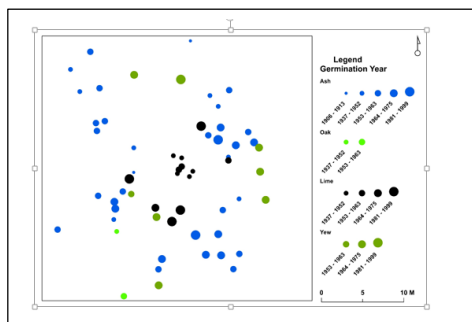

Figure 5. Proportional circles used to highlight the germination years of older and younger trees in the study area.
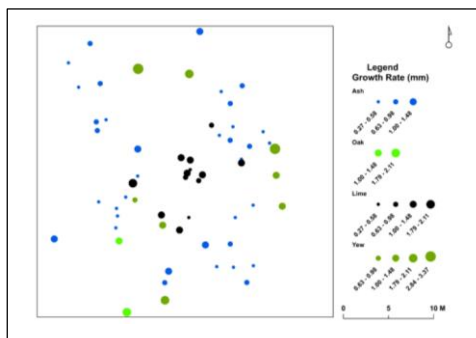

Figure 6. Average growth rates of all the trees surveyed at Heald Brow. Of particular interest are the faster growth rates of peripheral younger *T. cordata* satellite stems vis-a-vis the older central cluster of stems and also of *T. baccata*.
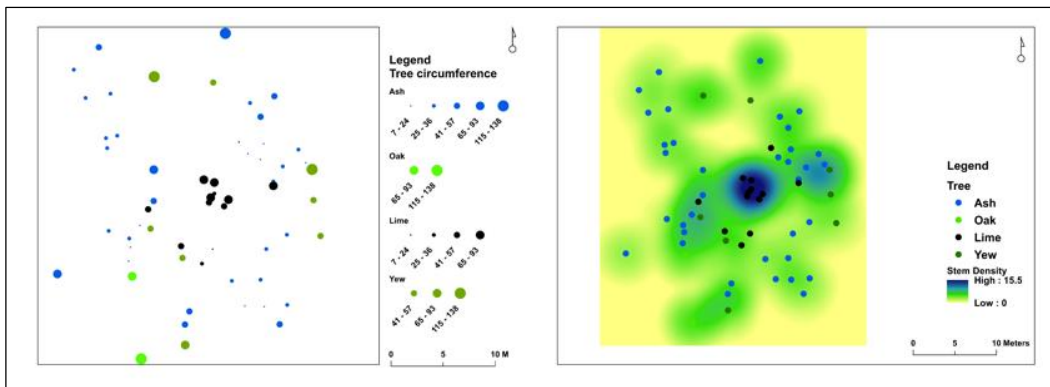
Figure 7a. Stem circumferences in AD 2011 across the study area. 7b. GIS Kernel Density analysis used to highlight the distribution of trees with large circumferences showing an apparent west-east pattern in stem density.
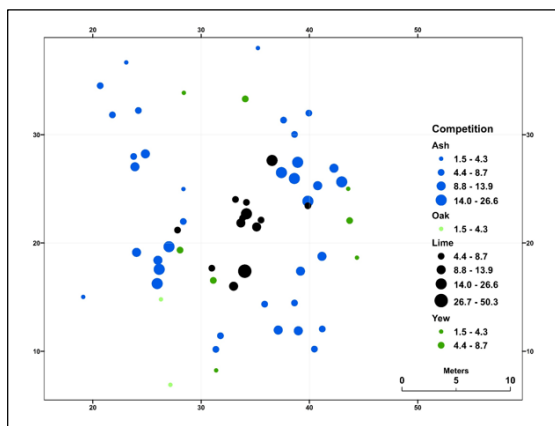

Figure 8. The degree of competition visualized across the study area using the competition intensity calculation of Anning and McCarthy (2013).

14